YTUP

Journal of Thermal Engineering
https://jten.yildiz.edu.tr/
https://doi.org/10.47481/jten.0048

RESEARCH ARTICLE

Analysis of thermodynamic characteristics of gas vessels under different conditions

Kangyu Deng[1,*], Xiaopeng Li[2,*], Wantong Wang[3]

[1]College of Civil Engineering, Hunan University, Changsha 410082, Hunan, China
[2]School of Emergency Management and Safety Engineering, China University of Mining and Technology-Beijing, Beijing 100083, China
[3]Department of Fire Command, China Fire and Rescue Institute, Beijing 102202, China

Abstract

With rapid industrial development, gas charging and discharging processes have become critical to energy storage systems. Current research predominantly focuses on specific vessel types or isolated operational stages and therefore lacks a unified thermodynamic framework that simultaneously addresses isochoric and isobaric constraints, heat transfer, adiabatic and isothermal processes, and the charging, storage, and discharging stages. Based on variable-mass thermodynamics theory, this study establishes a comprehensive modeling system comprising 18 distinct thermodynamic models that cover all combinations of these conditions and derives explicit analytical solutions in both differential and algebraic forms from fundamental conservation laws. Subsequently, specific case analyses are conducted for all thermodynamic models to assess differences among them, and their correctness is verified through numerical simulation; finally, the engineering implications, limitations, and applicability of the models are discussed. The results indicate that the isochoric adiabatic model exhibits relatively large variations in temperature and pressure, posing serious safety threats to material integrity; the isochoric heat transfer model is susceptible to ambient temperature effects and exhibits somewhat smaller temperature and pressure variations than the former; the isothermal model minimizes variations during the charging stage and restores initial conditions after discharging; and the isobaric model maintains constant temperature and pressure with only volume change, representing the ideal vessel type. This study comprehensively characterizes the thermodynamic behavior of gas vessels under varying conditions, providing a systematic theoretical basis for the engineering design of such vessels.

Keywords: Gas vessels, variable-mass thermodynamics, charging and discharging, gas storage

Cite this article as: Deng, K., Li, X., & Wang, W. (2026). Analysis of thermodynamic characteristics of gas vessels under different conditions. Journal of Thermal Engineering, 12(4), 1538–1557. https://doi.org/10.47481/jten.0048

1. Introduction

Thermodynamics, as a fundamental branch of physics, governs the energy conversion and transfer principles essential for engineering systems [1-2].In modern industrial applications, gas vessels serve as critical infrastructure for energy storage and supply, including high-pressure hydrogen tanks for fuel cell vehicles, compressed air energy storage (CAES) systems for grid-scale energy management, oxygen cylinders for medical and industrial use, and underground gas storage facilities for seasonal demand balancing. The thermodynamic behavior of these vessels during charging, storage, and discharging directly impacts the system efficiency, safety, and operational costs [3-6].

Engineering thermodynamics classifies gas vessels as either constant-mass or variable-mass systems [7-8]. Constant-mass systems maintain fixed gas quantities, with state changes driven by external boundary variations, which is a condition typical of static storage [9-10]. However, variable-mass systems experience dynamic mass inflow or outflow during charging and discharging, creating complex transient variations in temperature, pressure, and internal energy [11, 12]. The accurate prediction of these transients is essential for preventing material failure, optimizing filling protocols, and ensuring the operational safety of the reactor.

The growing emphasis on clean energy and efficient storage has intensified research into the thermodynamic behavior of gas vessels. Most studies have targeted specific applications.

*Corresponding Author
E-mail Adress: dky5646@hnu.edu.cn

Submitted: 21 November 2025;; **Accepted:** 28 March 2026

This paper was recommended for publication in revised form by Editor-in-Chief Ahmet Selim Dalkılıç

Research on fast-filling high-pressure hydrogen tanks commonly employs a simplified isochoric heat transfer model or isochoric adiabatic model to predict the internal temperature and pressure increase [13-17]. These models are limited to isochoric constraints and heat transfer calculations for the most part. They don't often look at how systems behave when they are working under isobaric conditions, or when there are complex dynamic boundaries. Isobaric storage chambers, in which the pressure is kept constant by hydraulic pistons or external pressure, have been considered in compressed air energy storage studies. Processes for near isothermal compression and expansion have been explored as well [18-22]. The results of these studies show that system performance is greatly affected by volume changes under constant pressure. But their models generally only look at one process at a time, such as charging, storage or discharging. They make the thermodynamic couplings within them too simple. This results in a lack of coherent characterization and mechanistic understanding of the inherent.

A comprehensive literature survey shows the following limitations of the present thermodynamic modeling of gas vessels:

1. Limited model coverage. Existing studies have typically focused on isolated configurations, either on constant-volume conditions for high-pressure cylinders or on constant-pressure systems for compressed air energy storage (CAES), without integrating these approaches into a unified framework. Within the existing frameworks, no comprehensive model exists that can simultaneously address mechanical constraints(isochoric/isobaric), thermal boundary conditions (heat transfer/adiabatic/isothermal), and operational stages (charging/storage/discharging).
2. Over-idealization. Many models assume adiabatic boundaries, although real systems transfer a lot of heat, or they assume that gases behave like ideal gases, ignoring the effects of compressibility at high pressures. Assuming a unit compressibility factor (Z=1) leads to large errors for high-pressure gases (e.g. 70 MPa hydrogen storage, or carbon dioxide at critical conditions) where Z corrections are required by real-gas equations of state (e.g. Peng-Robinson or Benedict-Webb-Rubin). It is very important to know the difference between quick near-adiabatic and slow near-isothermal processes when trying to predict temperature, but this is not always done well.
3. lack of analytical solution. Differential equations are often shown, but explicit algebraic solutions that can be used for direct engineering calculations have not been found very often. Complex or implicit solutions impede practical applications and parametric analyses.
4. Poor systematic derivations. Usually, the models are presented in their final form, without a detailed derivation from the conservation laws. This omission is detrimental to the understanding of the basic physical mechanisms and limits the extension or validation of the model.
5. Insufficient comparative analysis. Horizontal comparisons across different thermodynamic constraints and vertical analyses of the complete operational cycles are lacking. Consequently, model selection guidelines for specific engineering applications have not yet been developed.

In summary, to address limitations of current research, this study systematically investigated the thermodynamic characteristics of gas vessels under various thermodynamic states. This study, based on variable-mass thermodynamics theory, begins with three fundamental equations, namely, the gas state equation, the mass conservation equation, and the energy conservation equation, and, through rigorous mathematical derivation, establishes a thermodynamic modeling system for gas vessels comprising 18 scenarios. This system comprehensively covers the two fundamental constraints of isochoric and isobaric conditions, along with three typical thermal processes, including heat transfer, adiabatic, and isothermal conditions, while establishing the corresponding governing equations and analytical solutions for the three independent stages of charging, discharging, and storage. Through subsequent case studies and validation, we will compare in detail the dynamic responses and final states of various models under identical initial conditions, thereby elucidating the mechanisms by which different constraints and thermal processes influence the thermodynamic behavior of vessels during each of the independent stages of charging, storage, and discharging.

The main novelty of this study is threefold. First, considering different operating conditions and independent stages, 18 thermodynamic models covering all combinations of isochoric and isobaric constraints, heat-transfer, adiabatic, and isothermal processes, charging, storage, and discharging stages, are systematically derived. Second, it provides clear analytical solutions in both the differential and algebraic forms for all the models. Third, specific case analyses were conducted for all models, followed by in-depth comparisons and verifications. This study integrates charging, storage, and discharging into a complete dynamic process. This study provides a comprehensive theoretical foundation for the refined design, efficient operation, and performance optimization of gas vessels in energy and industrial applications.

2. Basic equation

2.1. Gas state equation

The state equations of gases are generally classified into two major categories: ideal gas state equations and real gas state equations [32-34]. The ideal-gas equation of state forms the basis for the real-gas equation of state; the latter is a derivative and a variation of the former in practical applications. We analyze these equations below.

The equation of state for an ideal gas relates to the variables pressure, volume, amount of substance, and temperature when the gas

is in stable equilibrium. This is established by Boyle's, Charles's, and Gay-Lussac's laws. The ideal gas equation of state was first proposed by Clapeyron; its core equation is as follows:

$$pV = nRT \quad (1)$$

Where p represents the pressure of an ideal gas, V represents the volume, n represents the amount of substance, T represents the thermodynamic temperature, and R is the universal gas constant (also known as the molar gas constant). It remains unchanged regardless of the molecular weight of the gas and has a value of 8.314 J/(mol·K). Four conclusions can be drawn from the above equation.

1. Boyle's law. When both n and T are constants, p is inversely proportional to V, and $pV = C_1$ .For further details, please refer to Figure 1.
2. Charles's law. When both n and V are constants, T is directly proportional to p, and $p/T = C_2$.
3. Gay-Lussac's law. When both p and n are constants, V is directly proportional to T, and $V/T = C_3$.
4. Avogadro's law. When both T and p are constants, V is directly proportional to n, and $V/n = C_4$.

where, C_1, C_2, C_3 and C_4 are all constants.

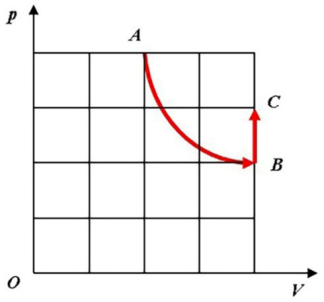

Figure 1. Boyle's law (inverse relationship of volume pressure)

The ideal gas state equation reveals the relationship among several variables of an ideal gas when it reaches a stable equilibrium state, including gas pressure, gas volume, amount of substance, and temperature. This is established based on Boyle's, Charles's, and Gay-Lussac's laws. The ideal gas state equation was first proposed by Clapeyron, and its core equation is as follows:

A→B is isothermal change, which is determined by Boyle's law: $p_A V_A = p_B V_B$.

B→C is an isochoric variation, which is determined by Charles' law: $p_B/T_B = p_C/T_C$.

Then, based on $T_A = T_B, V_B = V_C$, it can be concluded that $p_A V_A/T_A = p_C V_C/T_C$.

The actual gas state equation with the gas compression factor Z is expressed as follows:

$$pV = ZmRT \quad (2)$$

where, m is gas mass, kg. Z is the gas compression factor, which is conventionally 1 for an ideal gas.

By differentiating both sides, we obtain

$$\frac{dp}{p} + \frac{dV}{V} = \frac{dm}{m} + \frac{dT}{T} \quad (3)$$

To simplify calculations, the gas compression factor in this study is assumed to be 1 (Z=1). All subsequent theoretical derivations and calculations assume ideal gas. The ideal gas assumption is applicable at most pressures and temperatures significantly above the critical point, but not at high pressures.

2.2. Mass conservation equation

Using the control volume method, the mass conservation equation is derived as follows:

$$\frac{dm}{dt} = \dot{m}_{in} - \dot{m}_{out} - \dot{m}_{leakage} \quad (4)$$

where $\dot{m}_{in}$ is the mass flow rate of charging. $\dot{m}_{out}$ is the mass flow rate of discharging $\dot{m}_{leakage}$ is the mass flow rate of leakage.

For convenience in subsequent calculations, the differential equation can be transformed into an algebraic equation as follows:

From Eq. (4), the algebraic expression can be obtained as follows:

$$\delta m_{in} - \delta m_{out} - \delta m_{leakage} = dm \quad (5)$$

In the above mass conservation equation, it is assumed by default that δm_{in} , δm_{out} and $\delta m_{leakage}$ are all greater than 0.

When a completely sealed vessel is charging, $\delta m_{in} = dm$, At this point, $dm > 0$.

When a completely sealed vessel is discharging, $\delta m_{out} = dm$, At this point, $dm < 0$.

2.3. Energy conservation equation

The general form of the law of conservation of energy for a closed system is as follows:

$$\Delta E_{CV} = \delta Q - \delta W \quad (6a)$$

where, E_{CV} is total system energy J or kJ. Q is heat, J or kJ. W is the expansion work done on the surroundings, J or kJ.

$$\Delta E_{CV} = \delta Q + E_{in} - E_{out} - E_{leakage} - \delta W \quad (6b)$$

where, E_{in} is the energy flowing into the system, J or kJ. E_{out} is the energy flowing out the system, J or kJ. $E_{leakage}$ is the energy leaked from the system, J or kJ.

Expanding the above equation, we obtain

$$\frac{dU}{dt} = \dot{Q} + \left(h_{in} + \frac{1}{2}c_{in}^2 + gz_{in}\right)\dot{m}_{in} - \left(h_{out} + \frac{1}{2}c_{out}^2 + gz_{out}\right)(\dot{m}_{out} + \dot{m}_{leakage}) - \frac{dW}{dt} \quad (7)$$

where, U is thermodynamic energy, J or kJ. h_{in} is heat flow per unit time, J/s or kJ/s. is the enthalpy of the gas flowing into the system, J or kJ. h_{out} is the enthalpy of the gas flowing out of the system, J or kJ. c_{in} is the kinetic energy of the gas flowing into the system, J or kJ. c_{out} is the kinetic energy of the gas flowing out of the system, J or kJ. g is gravitational constant, N/kg. is the height of the charging port, m. z_{out} is the height of the discharging port, m.

Attention should be paid to the following.

$$\text{endothermic} \Leftrightarrow \delta Q = Q_{final} - Q_{start} > 0$$

$$\text{exothermic} \Leftrightarrow \delta Q = Q_{final} - Q_{start} < 0$$

$$\text{The system does work on the surroundings} \Leftrightarrow \delta W = W_{final} - W_{start} < 0$$

$$\text{Work done on the system by the surroundings} \Leftrightarrow \delta W = W_{final} - W_{start} > 0$$

where, Q_{final} is the initial heat of the system, J or kJ. Q_{start} is the final heat of the J or kJ. W_{final} is the mechanical work of the system at the final moment, J or kJ. W_{start} is the mechanical work of the system at the start moment, J or kJ.

When the system temperature is higher than the ambient temperature, the system dissipates heat; when the system temperature is lower than the ambient temperature, the system absorbs heat. For example, during the charging process, $\delta Q < 0$. When the system temperature is lower than the ambient temperature, heat is absorbed, for example, during the discharging $\delta Q > 0$ process. Because the velocity and positional (height) terms can be disregarded relative to enthalpy, this is also a uniform thermodynamic model. This simplification method significantly reduces the computational workload. Therefore, the above equation can be further simplified as follows:

$$\frac{dU}{dt} = \dot{Q} + h_{in}\dot{m}_{in} - h_{out}\left(\dot{m}_{out} + \dot{m}_{leakage}\right) - \frac{dW}{dt} \quad (8)$$

where, $\dot{Q} = h_{amb}A_{vessel}(T_{amb} - T)$, W or kW. h_{amb} is convective heat transfer coefficient, $W/(m^2 \cdot K)$. A_{vessel} is surface area of vessel, m^2

If the gas storage facility is completely sealed, the leakage term can be omitted, yielding the following equation:

$$\frac{dU}{dt} = \dot{Q} + h_{in}\dot{m}_{in} - h_{out}\dot{m}_{out} - \frac{dW}{dt} \quad (9a)$$

In addition, the following equations apply:

$$dU = mc_p dT + c_p T dm - pdV - Vdp \quad (9b)$$

$$\begin{cases} c_p - c_v = R \\ \frac{c_p}{c_v} = k \end{cases} \Rightarrow \begin{cases} c_v = \frac{kR}{k-1} \\ c_v = \frac{R}{k-1} \end{cases} \quad (9c)$$

where,c_p is specific heat capacity at isobaric, kJ/(kg·K). c_v is specific heat capacity at constant volume, kJ/(kg·K). k is the adiabatic index, which is generally 1.4.

Substituting the above equation into equation (9a), and because of $dm/dt = \dot{m}_{in} - \dot{m}_{out}$ and $\dot{W} = pdV/dt$, we obtain:

$$mc_p\frac{dT}{dt} = \dot{Q} + \dot{m}_{in}c_p(T_{in} - T) + \dot{m}_{out}c_p(T - T_{out}) + V\frac{dp}{dt} \quad (10)$$

The above equation represents the energy conservation equation for open systems in both its mass and differential forms.

3. Thermodynamic model of gas vessels under different conditions

The thermodynamic model of gas vessels is established by combining the three fundamental equations from the previous section: the gas state equation, the mass conservation equation, and the energy conservation equation. In the energy conservation equation, both dT/dt and dp/dt appear; these are the rates of change of temperature and pressure and are the key unknown variables. By combining the dm/dt term in the mass form of the mass conservation equation with the gas state equation, the three unknown variables m, T, and p can be solved. The mass form of the vessel thermodynamic model is adopted in this study and in the subsequent theoretical derivations.

Variable-mass thermodynamics analyzes open systems in which mass crosses the system boundaries, in contrast to constant-mass thermodynamics. For gas vessels undergoing charging or discharging, the control-volume approach is essential: the vessel constitutes a control volume with mass flow across its inlet and outlet boundaries, while energy transfers occur as enthalpy flow associated with mass transfer, heat transfer across vessel walls, and boundary work in deformable control volumes.

For the gas vessel analysis, we employ a lumped-parameter assumption in which intensive properties, such as temperature, pressure, and density, are uniform throughout the vessel volume at any instant. This assumption is valid under the following two conditions. First, the vessel dimensions are small compared to the thermal diffusion length scales, and the Biot number is less than 0.1. Sec-

ond, internal mixing is strong due to inlet jet turbulence. Under this framework, we derive system-scale governing equations from the gas state equation, the law of mass conservation, and the law of energy conservation. As shown in Figure 2, general thermodynamic models of sealed vessels can be classified into two types.

1. Isochoric model
2. Isobaric model

Based on the above, if heat transfer, adiabatic conditions, and isothermal conditions are considered simultaneously, the thermodynamic models can be classified into six types.

1. VH model: Isochoric heat transfer model
2. VA model: isochoric adiabatic model
3. VT model: isochoric isothermal model
4. PH model: isobaric heat transfer model
5. PA model: isobaric adiabatic model
6. PT model: isobaric isothermal model

If charging, discharging, and storage are considered simultaneously, the general thermodynamic model of a sealed vessel can be classified into 18 types based on the above.

1. VHC model: isochoric heat transfer and charging model
2. VHD model: isochoric heat transfer and discharging model
3. VAC model: isochoric adiabatic and charging model
4. VAD model: isochoric adiabatic and discharging model
5. VTC model: isochoric isothermal and charging model
6. VTD model: isochoric isothermal and discharging model
7. PHC model: isobaric heat transfer and charging model
8. PHD model: isobaric heat transfer and discharging model
9. PAC model: isobaric adiabatic and charging model
10. PAD model: isobaric adiabatic and discharging model
11. PTC model: isobaric isothermal and charging model
12. PTD model: isobaric isothermal and discharging model
13. VHS model: isochoric heat transfer and storage model
14. VAS model: isochoric adiabatic and storage model
15. VTS model: isochoric isothermal and storage model
16. PHS model: isobaric heat transfer and storage model
17. PAS model: isobaric adiabatic and storage model
18. PTS model: isobaric isothermal and storage model

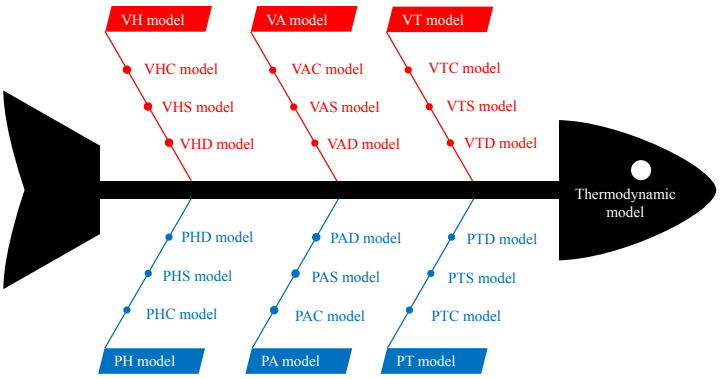

Figure 2. Classification of thermodynamic models

Table 1. Timetable for gas vessels

State / Variable	t_0 (Starting time)	t (End time)	Charging	Discharging
Temperature	T_0	T	T_{in}	T_{out}
Pressure	p_0	p	p_{in}	p_{out}
Mass	m_0	m	m_{in}	m_{out}
Volume	V_0	V		

The thermodynamic parameters of the gas vessels were defined prior to the analysis of the thermodynamic model. The details are presented in Table 1.

3.1. Isochoric heat transfer and charging model (VHC model)

Regarding the charging state, equation (10), the state equation of energy conservation, becomes:

$$mc_p \frac{dT}{dt} = \dot{Q} + \dot{m}_{in} c_p (T_{in} - T) + V \frac{dp}{dt} \tag{11}$$

The differential form of the thermodynamic model can be derived from the differential form of the combined gas state equation, as follows:

$$\begin{cases} \dfrac{dp}{dt} = \dfrac{(k-1)\dot{Q} + k\dot{m}_{in} R T_{in}}{V} \\ \dfrac{dT}{dt} = \dfrac{\dot{Q} + c_p \dot{m}_{in} T_{in} - c_v \dot{m}_{in} T}{c_v m} \\ \dfrac{dV}{dt} = 0 \end{cases} \tag{12}$$

The analytical solution for equation (12) is provided in the appendix at the end of this article.

3.2. Isochoric heat transfer and discharging model (VHD model)

Because it is in a discharging state, equation (10), the energy conservation state equation, transforms into the following form:

$$mc_p \frac{dT}{dt} = \dot{Q} + \dot{m}_{out} c_p (T - T_{out}) + V \frac{dp}{dt} \tag{13}$$

By combining the differential form of the gas state equation, we obtain:

$$\begin{cases} \frac{dp}{dt} = \frac{(k-1)\dot{Q} - \dot{m}_{out} RkT}{V} \\ \frac{dT}{dt} = \frac{k\dot{Q} - \dot{m}_{out} RkT}{mc_p} \\ \frac{dV}{dt} = 0 \end{cases} \tag{14}$$

The analytical solution for equation (14) is provided in the appendix at the end of this article.

3.3. Isochoric Adiabatic and Charging Model (VAC model)

Because it is in an adiabatic state, equation (12) changes to the following form:

$$\begin{cases} \frac{dp}{dt} = \frac{k\dot{m}_{in} RT_{in}}{V} \\ \frac{dT}{dt} = \frac{k\dot{m}_{in} T_{in} - \dot{m}_{in} T}{m} \\ \frac{dV}{dt} = 0 \end{cases} \tag{15}$$

By using the variable separation method to solve the above equation, we can obtain:

$$\begin{cases} p = p_0 + \frac{k\dot{m}_{in} RT_{in}}{V}(t - t_0) \\ T = \frac{m_0 T_0 + kT_{in}\dot{m}_{in}(t - t_0)}{\dot{m}_{in}(t - t_0) + m_0} \\ V = V_s \end{cases} \tag{16}$$

Note that in the above equation, t represents time and is located after the t_0 moment.

Continuing the derivation, we obtain the ordinary algebraic expression:

$$\begin{cases} p = p_0 + \frac{k\dot{m}_{in} RT_{in}}{V} t \\ T = \frac{m_0 T_0 + kT_{in}\dot{m}_{in} t}{\dot{m}_{in} t + m_0} \\ V = V_s \end{cases} \tag{17}$$

Note: t represents the period.

3.4. Isochoric adiabatic and discharging model (VAD model)

Because it is in an adiabatic state, equation (14) changes to the following form:

$$\begin{cases} \frac{dp}{dt} = \frac{\dot{m}_{out} RkT}{V} \\ \frac{dT}{dt} = \frac{\dot{m}_{out}(k-1)T}{m} \\ \frac{dV}{dt} = 0 \end{cases} \tag{18}$$

By using the variable separation method to solve the above equation, we can obtain:

$$\begin{cases} p = p_0 \left(\frac{m_0 - \dot{m}_{out}(t - t_0)}{m_0} \right)^k \\ T = T_0 \left(\frac{m_0 - \dot{m}_{out}(t - t_0)}{m_0} \right)^{k-1} \\ V = V_s \end{cases} \tag{19}$$

Note that in the above equation, t represents time and is located after the t_0 moment.

Thus, the general algebraic expression can be obtained as follows:

$$\begin{cases} p = p_0 \left(\frac{m_0 - \dot{m}_{out} t}{m_0} \right)^k \\ T = T_0 \left(\frac{m_0 - \dot{m}_{out} t}{m_0} \right)^{k-1} \\ V = V_s \end{cases} \tag{20}$$

Note: t represents the period.

3.5. Isochoric isothermal and charging model (VTC model)

Because it is an isothermal state, equation (10) becomes:

$$\dot{Q} + \dot{m}_{in} c_p (T_{in} - T) + V \frac{dp}{dt} = 0 \tag{21}$$

From the gas state equation under isothermal and isochoric conditions, the following equation is obtained:

$$\frac{dp}{dt} = \frac{RT}{V} \dot{m}_{in}$$

By combining the two equations, we obtain the following:

$$Q = \frac{V}{k-1} \left(1 - k \frac{T_{in}}{T} \right) (p_2 - p_1) \tag{22}$$

Thus, the magnitude of heat transfer during isothermal charging is directly proportional to the pressure difference in the storage tank between the states before and after the process. The sign of the heat transfer during isothermal charging depends on the size of $(1 - kT_{in}/T)$. The specific analyses are as follows:

- When $T_{in} > T/k, Q < 0$, and the system releases heat to the surroundings.
- When $T_{in} = T/k, Q = 0$, the system is thermally insulated

from the surroundings.

- When $T_{in} < T/k, Q > 0$, the system absorbs heat from the surroundings.

The final equation is as follows:

$$\begin{cases} \frac{dp}{dt} = \frac{RT}{V}\dot{m}_{in} \\ \frac{dT}{dt} = 0 \\ \frac{dV}{dt} = 0 \end{cases} \quad (23)$$

3.6. Isochoric isothermal and discharging model (VTD model)

Because it is an isothermal state, equation (10) becomes

$$\dot{Q} + \dot{m}_{out\backslash} c_p (T - T_{out\backslash}) + V\frac{dp}{dt} = 0 \quad (24)$$

The reasoning process is the same as that described above, and the final equation can be obtained as:

$$\begin{cases} \frac{dp}{dt} = -\frac{RT}{V}\dot{m}_{out} \\ \frac{dT}{dt} = 0 \\ \frac{dV}{dt} = 0 \end{cases} \quad (25)$$

3.7. Isobaric heat transfer and charging model (PHC model)

Under isobaric heat transfer and the charging state, equation (10) becomes

$$mc_p\frac{dT}{dt} = \dot{Q} + \dot{m}_{in} c_p (T_{in} - T) \quad (26)$$

By combining the differential form of the gas state equation, we obtain the following:

$$\begin{cases} \frac{dp}{dt} = 0 \\ \frac{dT}{dt} = \frac{\dot{Q} + \dot{m}_{in} c_p (T_{in} - T)}{mc_p} \\ \frac{dV}{dt} = \frac{(k-1)\dot{Q} + \dot{m}_{in} kRT_{in}}{kp} \end{cases} \quad (27)$$

3.8. Isobaric heat transfer and discharging model (PHD model)

Because it is an isobaric heat transfer and discharging state, equation (10) becomes

$$mc_p\frac{dT}{dt} = \dot{Q} + \dot{m}_{out} c_p (T - T_{out}) \quad (28)$$

The reasoning process is the same as that described above, and the final equation can be obtained as

$$\begin{cases} \frac{dp}{dt} = 0 \\ \frac{dT}{dt} = \frac{\dot{Q}}{mc_p} \\ \frac{dV}{dt} = \frac{(k-1)\dot{Q} - \dot{m}_{out} kRT}{kp} \end{cases} \quad (29)$$

3.9. Isobaric adiabatic and charging model (PAC model)

Because it is an isobaric adiabatic and charging state, equation (27) becomes

$$\begin{cases} \frac{dp}{dt} = 0 \\ \frac{dT}{dt} = \frac{\dot{m}_{in}(T_{in} - T)}{m} \\ \frac{dV}{dt} = \frac{\dot{m}_{in} RT_{in}}{p} \end{cases} \quad (30)$$

3.10. Isobaric adiabatic and discharging model (PAD model)

Because it is an isobaric adiabatic and discharging state, equation (29) becomes

$$\begin{cases} \frac{dp}{dt} = 0 \\ \frac{dT}{dt} = 0 \\ \frac{dV}{dt} = \frac{-\dot{m}_{out} RT}{p} \end{cases} \quad (31)$$

3.11. Isobaric isothermal and charging model (PTC model)

Because it is an isobaric isothermal and charging state, equation (10) becomes

$$\dot{Q} + \dot{m}_{in} c_p (T_{in} - T) = 0 \quad (32)$$

Combining the differential form of the gas state equation, then setting and , the derivation can be obtained as follows:

$$\begin{cases} \frac{dp}{dt} = 0 \\ \frac{dT}{dt} = 0 \\ \frac{dV}{dt} = \frac{\dot{m}_{in} RT_s}{p_s} \end{cases} \quad (33)$$

3.12. Isobaric isothermal and discharging model (PTD model)

Because it is an isothermal, isobaric, and discharging state, equation (10) becomes

$$\dot{Q} + \dot{m}_{out} c_p (T - T_{out}) = 0 \quad (34)$$

Combining the differential form of the gas state equation and setting $p = p_s$ and $T = T_s$, the derivation can be obtained as follows:

$$\begin{cases} \frac{dp}{dt} = 0 \\ \frac{dT}{dt} = 0 \\ \frac{dV}{dt} = \frac{-\dot{m}_{out} R T_s}{p_s} \end{cases} \quad (35)$$

3.13. Isochoric heat transfer and storage model (VHS model)

During the gas storage stage, convective heat transfer occurs between the air and the vessel wall; thus,

$$\dot{Q} = h_{amb} A_{vessel} (T_{amb} - T) \quad (36)$$

If $T > T_{amb}$, then the $\dot{Q} < 0$ system is in a state of heat release. According to the ideal gas equation pV=mRT , as the system temperature decreases, the pressure decreases.

If $T < T_{amb}$, then $\dot{Q} > 0$ the system is in a state of heat absorption. According to the ideal gas law pV=mRT , if the system temperature increases, the pressure increases accordingly.

From equation (10), the energy conservation equation under isochoric conditions of heat transfer and storage is obtained as follows:

$$mc_p \frac{dT}{dt} = \dot{Q} + V \frac{dp}{dt} \quad (37)$$

By combining the gas state equation, we obtain the following:

$$\begin{cases} \frac{dp}{dt} = \frac{(k-1)\dot{Q}}{V} \\ \frac{dT}{dt} = \frac{\dot{Q}}{mc_v} \\ \frac{dV}{dt} = 0 \end{cases} \quad (38)$$

By continuing to employ the method of separation of variables, we can obtain analytical solutions for pressure, temperature, and volume in the isochoric heat transfer and storage model (VHS model). The results are as follows:

$$\begin{cases} p = \frac{mR}{V}\left(T_{amb} + \frac{T_0 - T_{amb}}{e^{\frac{c_v m(t-t_0)}{h_{amb} A_{vessel}}}}\right) \\ T = T_{amb} + \frac{T_0 - T_{amb}}{e^{\frac{c_v m(t-t_0)}{h_{amb} A_{vessel}}}} \\ V = V_s \end{cases} \quad (39)$$

Continuing the derivation, we obtain the ordinary algebraic expression:

$$\begin{cases} p = \frac{mR}{V}\left(T_{amb} + \frac{T_0 - T_{amb}}{e^{\frac{c_v mt}{h_{amb} A_{vessel}}}}\right) \\ T = T_{amb} + \frac{T_0 - T_{amb}}{e^{\frac{c_v mt}{h_{amb} A_{vessel}}}} \\ V = V_s \end{cases} \quad (40)$$

Note: t represents the period.

3.14. Isochoric adiabatic and storage model (VAS model)

For a closed system, the energy conservation equation is expressed as dU = Q -W. Since it is adiabatic and isochoric, both Q and W are 0; thus, dU = 0. All thermodynamic variables at the end of storage are identical to those at the beginning, indicating that the state of the isobaric heat-transfer storage is also isothermal. Therefore, we have:

$$\begin{cases} p = p_0 \\ T = T_0 \\ V = V_s \end{cases} \quad (41)$$

3.15. Isochoric isothermal and storage model (VTS model)

From equation (10), the energy conservation equation under isochoric, isothermal, and storage conditions can be obtained as follows:

$$0 = \dot{Q} + V \frac{dp}{dt} \quad (42)$$

Further derivation yields the following equation:

$$\frac{dp}{dt} = -\frac{\dot{Q}}{V} \quad (43)$$

Then we have:

$$\begin{cases} \frac{dp}{dt} = -\frac{\dot{Q}}{V} \\ \frac{dT}{dt} = 0 \\ \frac{dV}{dt} = 0 \end{cases} \quad (44)$$

3.16. Isobaric heat transfer and storage model (PHS model)

From equation (10), the energy conservation equation under isobaric heat transfer and storage conditions can be obtained as follows:

$$mc_p \frac{dT}{dt} = \dot{Q} \quad (45)$$

Combining the differential form of the gas state equation with equation (36) yields the following derivation:

$$\begin{cases} \frac{dp}{dt} = 0 \\ \frac{dT}{dt} = \frac{h_{amb} A_{vessel} (T_{amb} - T)}{c_p m} \\ \frac{dV}{dt} = \frac{R h_{amb} A_{vessel} (T_{amb} - T)}{c_p p} \end{cases} \quad (46)$$

By employing the method of separation of variables, we obtain analytical solutions for the isobaric heat transfer and storage model (PHS model): pressure, temperature, and volume. The results are as follows:

$$\begin{cases} p = p_0 \\ T = \frac{T_0 - T_{amb}}{e^{\frac{h_{amb} A_{vessel}(t-t_0)}{c_p m}}} + T_{amb} \\ V = \frac{mR}{p}\left(\frac{T_0 - T_{amb}}{e^{\frac{h_{amb} A_{vessel}(t-t_0)}{c_p m}}} + T_{amb}\right) \end{cases} \quad (47)$$

Further derivation yields the following ordinary algebraic expression for the thermodynamic model:

$$\begin{cases} p = p_0 \\ T = \dfrac{T_0 - T_{amb}}{e^{\frac{h_{amb} A_{vessel} t}{c_p m}}} + T_{amb} \\ V = \dfrac{mR}{p}\left(\dfrac{T_0 - T_{amb}}{e^{\frac{h_{amb} A_{vessel} t}{c_p m}}} + T_{amb} \right) \end{cases} \quad (48)$$

Note: t represents the period.

3.17. Isobaric adiabatic and storage model (PAS model)

From equation (47), the energy conservation equation under isobaric adiabatic and storage conditions can be obtained as follows:

$$\begin{cases} p = p_0 \\ T = T_0 \\ V = \dfrac{mR}{p} T_0 = V_0 \end{cases} \quad (49)$$

The above equation shows that all thermodynamic variables at the end of storage are the same as those at the beginning of storage; that is, the isobaric heat-transfer storage state is also isothermal.

3.18. Isobaric isothermal and storage model (PTS model)

From equation (10), the energy conservation equation under isobaric and isothermal storage conditions can be obtained as follows:

$$\dot{Q} = 0 \quad (50)$$

According to the time differential form of the gas state equation, we can obtain $dV/dt = (RTdm/dt + mRdT/dt - Vdp/dt)/p.$. Since it is isobaric isothermal state and $dm/dt = 0$, then:

$$\frac{dV}{dt} = 0 \quad (51)$$

Then we can obtain:

$$\begin{cases} \dfrac{dp}{dt} = 0 \\ \dfrac{dT}{dt} = 0 \\ \dfrac{dV}{dt} = 0 \end{cases} \quad (52)$$

If it is transformed into an algebraic expression, then

$$\begin{cases} p = p_0 \\ T = T_0 \\ V = V_0 \end{cases} \quad (53)$$

4. Case analysis and validation

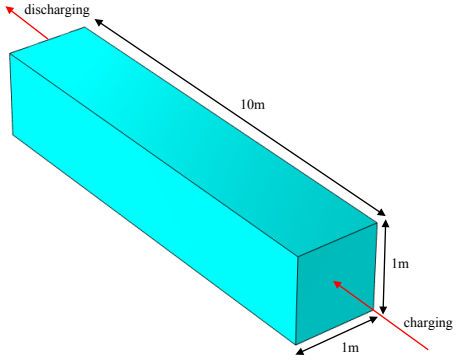

Figure 3. Schematic diagram of gas vessels

Table 2. Initial parameter values of the model

Initial parameters	Value
Initial temperature (T_0)	293.15 K(20 °C)
Initial air pressure (p_0)	101325 Pa(1atm)
Initial volume (V_0)	10 m^3
Charging temperature (T_{in})	293.15 K(20 °C)
Disharging pressure (p_{in})	0.2 MPa
Ambient temperature (T_0)	293.15 K(20 °C)
Ambient pressure (p_0)	101325 Pa(1 atm)
The mass flow rate of charging ($\dot{m}_{in}$)	0.1 kg/s
The mass flow rate of discharging ($\dot{m}_{out}$)	0.1 kg/s
Vessel surface area (A_{vessel})	42 m^2
Convective heat transfer coefficient (h_{amb})	5 W/(m^2·K)

For computational convenience, the gas vessels are modeled as rectangular prisms with a square cross-section of 1m * 1m and a length of 10 m. The gas is introduced through the right cross-section and discharged through the left cross-section, as shown in Figure 3. A complete storage-discharge cycle is considered the object of analysis. Thus, the overall thermodynamic model of the gas vessels is divided into six types: isochoric heat transfer (VH), isochoric adiabatic (VA), isochoric isothermal (VT), isobaric heat transfer (PH), isobaric adiabatic (PA), and isobaric isothermal (PT) models. The parameters are set as shown in Table 2; that is, the initial parameters of all thermodynamic models are the same, and differences among the models are studied.

4.1. Isochoric model

The isochoric model of gas vessels is generally divided into three types: heat transfer, adiabatic, and isothermal. The isochoric heat transfer model describes heat exchange between the vessel surface and the external environment. The isochoric adiabatic model is usually characterized by rapid charging and discharging; during charging, discharging, and storage, there is no heat transfer between the vessel surface and the external environment. The isochoric isothermal model is typically characterized by slow charging and dis-

charging, implying that during these processes the vessels exchange sufficient heat with the external environment. Therefore, the vessels' internal temperature generally corresponds to the external temperature.

4.1.1. Isochoric heat transfer model (VH model)

According to the VH model presented in the previous section, the initial parameters in Table 2 are substituted into the VH model to calculate the variation laws throughout the entire isochoric heat transfer process. Figures 4-6 show the results. As shown in Figure 4, during the charging stage the pressure increased linearly to 171,977.6 Pa (1.7 atm) and remained constant during the storage stage; it then decreased linearly to 127,542 Pa (1.26 atm) during the discharging stage. As shown in Figure 5, during the charging stage, the temperature slightly increased to 293.19 K (20.04 ℃), returned to the ambient temperature of 293.15 K (20 ℃) during the storage stage, and then sharply decreased to 257.9 K (−15.25 ℃) during the discharging stage. As shown in Figure 6, the volume remains unchanged throughout the process because the model is isochoric.

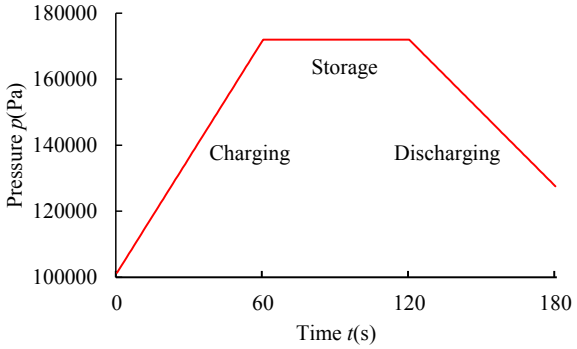

Figure 4. pressure changes throughout the Isochoric heat transfer process

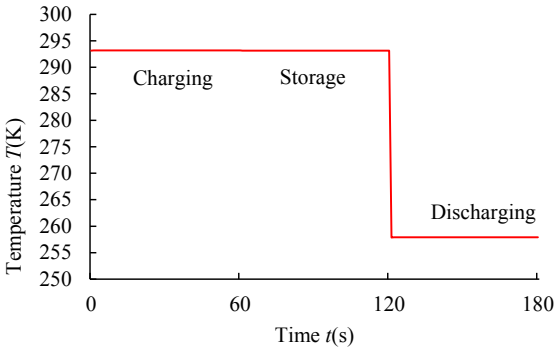

Figure 5. temperature changes throughout the isochoric heat transfer process

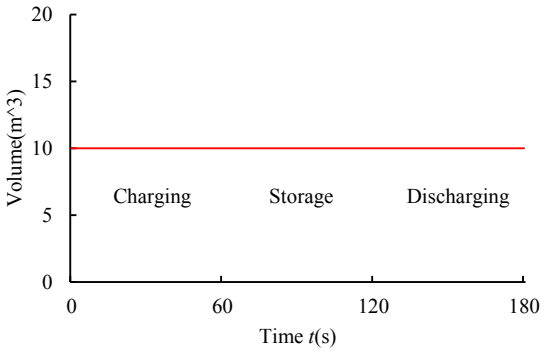

Figure 6. volume changes throughout the isochoric heat transfer process

4.1.2. Isochoric adiabatic model (VA model)

Using the VA model presented in the previous section, the initial parameters in Table 2 are substituted to calculate the variation rules throughout the entire isochoric adiabatic process. The results are shown in Figures 7, 8, and 9. Figure 7 shows that during the charging stage the pressure gradually rises to 171,977.6 Pa (1.7 atm) and then remains constant during the storage stage. During the discharging stage, the pressure decreases linearly to 97,637.76 Pa (0.96 atm). Theoretically, when the discharge time reaches 56.77 s, the pressure decreases to atmospheric (ambient) pressure, and the vessels stop discharging. However, if forced evacuation is performed (like vacuuming), the internal pressure of the vessels can be reduced below atmospheric pressure.

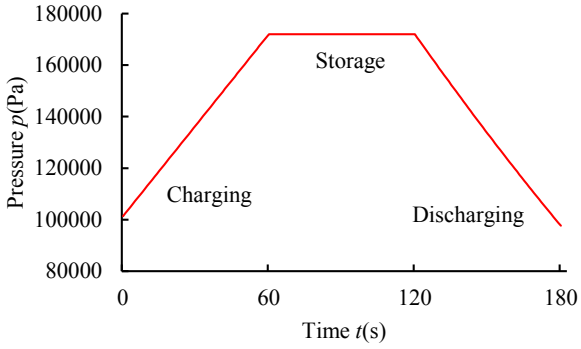

Figure 7. pressure changes in the entire isochoric adiabatic process

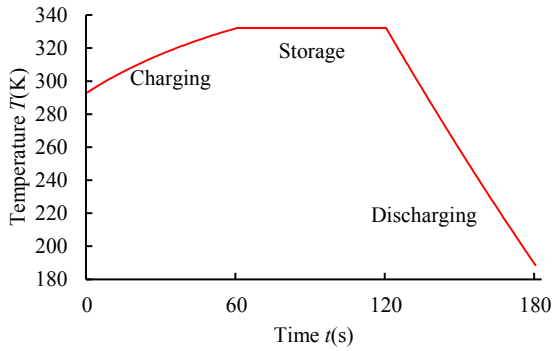

Figure 8. temperature changes in the entire isochoric adiabatic process

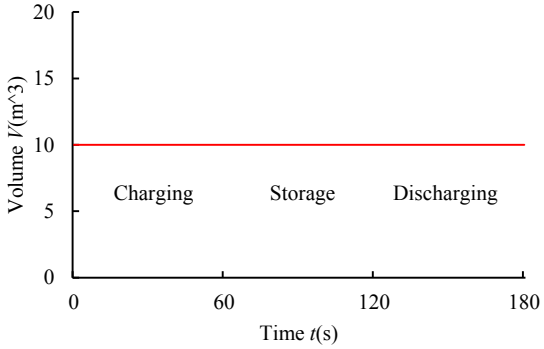

Figure 9. volume changes in the entire isochoric adiabatic process

Figure 8 shows that during the charging stage the temperature increases linearly to 332.15 K (59 °C) and then remains constant during the storage stage. During the discharging stage, the temperature drops sharply to 188.57 K (-84.58 °C). If the cut-offline is set at atmospheric pressure, that is, when the discharge time reaches 56.77 s, the temperature inside the vessels is 195.7 K (-77.45 °C). As shown in Figure 9, the volume remains unchanged throughout the process because the model is isochoric.

4.1.3. Isochoric isothermal model (VT model)

According to the VT model in the previous section, the initial parameters in Table 2 are substituted to calculate the variation rules throughout the entire process of the isochoric and isothermal model (VT model). The results are shown in Figures 10, 11, and 12. By observing Figure 10, it can be found that during the charging stage, the pressure linearly rises to 151805.43 Pa (1.5 atm), then remains constant during the storage stage, and in the discharging stage, the pressure linearly drops to the atmospheric pressure level. By observing Figure 11 and Figure 12, it can be found that since it is isochoric isothermal model (VT model), the temperature and volume remain unchanged throughout the entire process.

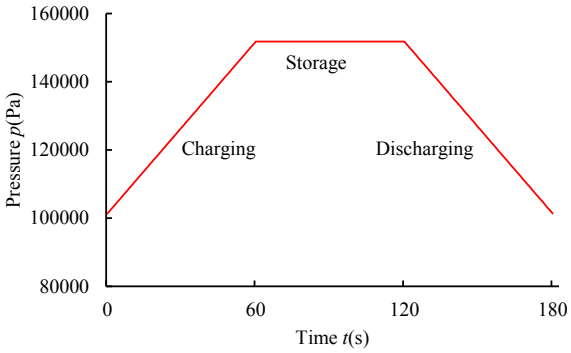

Figure 10. pressure changes in the entire process of isochoric and isothermal conditions

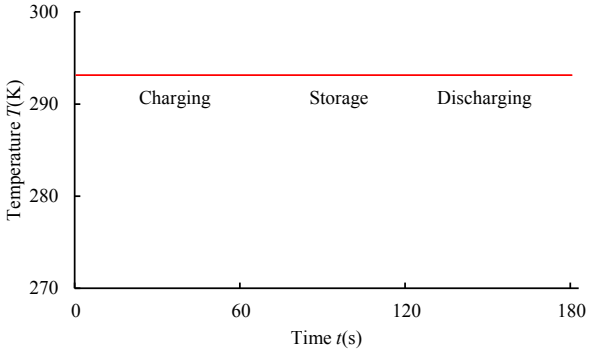

Figure 11. temperature changes in the entire process of isochoric and isothermal conditions

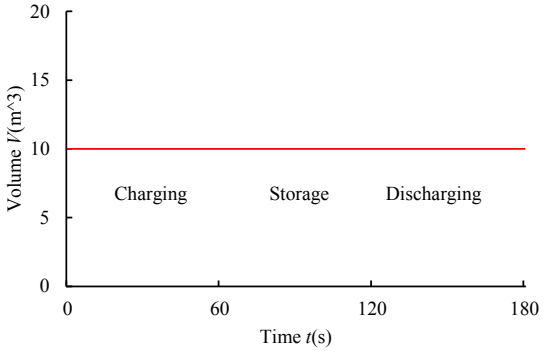

Figure 12. Volume changes in the entire process of isochoric and isothermal conditions

4.2. Isobaric nodel

The isobaric model of gas vessels is divided into three types: the isobaric heat transfer model, the isobaric adiabatic model, and the isobaric isothermal model. The isobaric model is analogous to a piston compressor, in which the gas vessels remain isobaric throughout the process. Among these, the isobaric heat transfer model is analogous to a piston compressor, which involves heat exchange with the surroundings. By contrast, isobaric adiabatic model assumes that the

gas vessels do not exchange heat with the surroundings during the entire process and is characteristic of rapid charging and discharging. The isobaric isothermal model corresponds to slow charging and discharging and is consistent with the isochoric model. Moreover, during the charging and discharging processes of the isobaric model, the volumes of the gas vessels change. The initial volume of the gas vessels remains 10 m^3, equal to that of the isochoric model. Therefore, the parameters of the gas vessels in the isobaric model are presented in Figure 3 and Table 2.

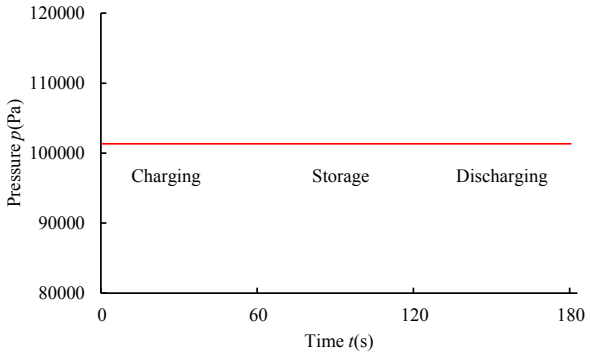

Figure 13. The pressure variation throughout the entire process of the isobaric model

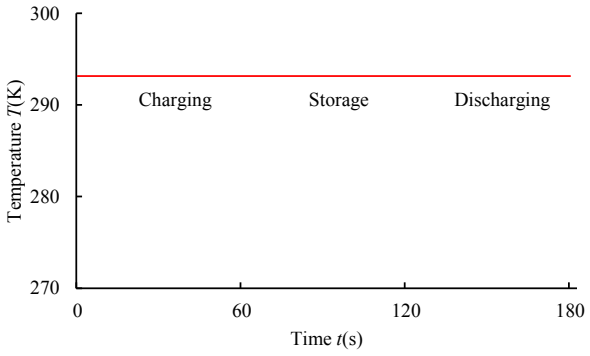

Figure 14. The temperature variation throughout the entire process of the isobaric model

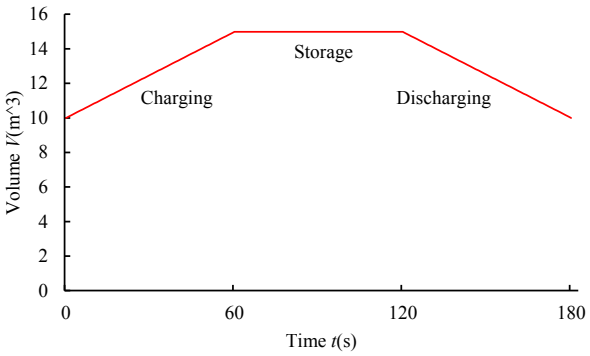

Figure 15. The volume variation throughout the entire process of the isobaric model

According to the conclusion of the previous section, the variation laws throughout the entire process of the isobaric heat transfer model, the isobaric adiabatic model, and the isobaric isothermal model are calculated by substituting the initial parameters in Table 2. The results are consistent. This is because the intake temperature, the initial temperature of the vessels, the ambient temperature are identical, and no heat transfer occurs between the gas vessels and the external environment. Moreover, the models are isobaric. The graphs of the resulting data of the three isobaric models are identical, as shown in Figures 13-15. As shown in Figures 13 and 14, the pressure and temperature of the gas remained constant throughout the entire process. As shown in Figure 15, the volume of the gas vessels increased linearly to 14.98 m^3 during the charging stage, remained unchanged during the storage stage, and decreased to 10 m^3 during the discharging stage, which was the initial volume.

4.3. Comparative analysis of models

To facilitate comparison among all thermodynamic models, the case data presented above are summarized in Table 3. The following findings were observed:

1. The results of the VH and VA models are identical during both the charging and storage stages. However, the gas pressure and temperature following discharge from the VH model are higher than in the VA model. The VH model absorbs heat from the environment via convective heat transfer in the vessels during the final discharge stage.
2. The temperature and pressure at the end of charging in the VT model are lower than those in the VH and VA models. However, at the end of discharge, both the temperature and pressure return to their initial levels.
3. The PH, PA, and PT models (three isobaric models) exhibit identical results throughout the process. In the isobaric models, pressure and temperature remain constant at their initial values, and only the volume changes.
4. The volume of the isochoric model remains unchanged throughout the process, while the volume of the isobaric model varies between 10 m^3 and 14.98 m^3.

Table 3: Model results

Moment / Variable	t_0	t_1	t_2	t_3
p of VH model	101325Pa(1atm)	171977.6Pa(1.7atm)	171977.6Pa(1.7atm)	127542Pa(1.26atm)
p of VA model	101325Pa(1atm)	171977.6Pa(1.7atm)	171977.6Pa(1.7atm)	97637.76Pa(0.96atm)
p of VT model	101325Pa(1atm)	151805.43 Pa (1.5atm)	151805.43 Pa (1.5atm)	101325Pa(1atm)
p of PH model	101325Pa(1atm)	101325Pa(1atm)	101325Pa(1atm)	101325Pa(1atm)
p of PA model	101325Pa(1atm)	101325Pa(1atm)	101325Pa(1atm)	101325Pa(1atm)
p of PT model	101325Pa(1atm)	101325Pa(1atm)	101325Pa(1atm)	101325Pa(1atm)
T of VH model	293.15K(20°C)	293.19K(20.04°C)	293.15K(20°C)	257.9K(-15.25°C)
T of VA model	293.15K(20°C)	332.15K(59°C)	332.15K(59°C)	188.57K(-84.58°C)
T of VT model	293.15K(20°C)	293.15K(20°C)	293.15K(20°C)	293.15K(20°C)
T of PH model	293.15K(20°C)	293.15K(20°C)	293.15K(20°C)	293.15K(20°C)
T of PA model	293.15K(20°C)	293.15K(20°C)	293.15K(20°C)	293.15K(20°C)
T of PT model	293.15K(20°C)	293.15K(20°C)	293.15K(20°C)	293.15K(20°C)
V of VH model	10 m^3	10 m^3	10 m^3	10 m^3
V of VA model	10 m^3	10 m^3	10 m^3	10 m^3
V of VT model	10 m^3	10 m^3	10 m^3	10 m^3
V of PH model	10 m^3	14.98 m^3	14.98 m^3	10 m^3
V of PA model	10 m^3	14.98 m^3	14.98 m^3	10 m^3
V of PT model	10 m^3	14.98 m^3	14.98 m^3	10 m^3

Here, t_0 represents the zero moment, that is, the moment when charging begins; t_1 represents the moment when charging ends and storage begins simultaneously; t_2 represents the moment when storage ends and discharging begins simultaneously; and t_3 represents the moment when discharging ends.

4.4. Model validation

To quickly verify the correctness of the theoretical model, the isochoric heat transfer and charging model (VAC model) is selected from among 18 thermodynamic models for numerical simulation. The simulation is conducted using COMSOL software, employing two physics interfaces: laminar flow and fluid heat transfer. These two physical fields are coupled in a non-isothermal flow. The initial parameters for the simulation are consistent with those listed in

ble 2. The inlet is in the lower right corner, and the outlet is in the upper left corner. The inflation time is set to 60 s.

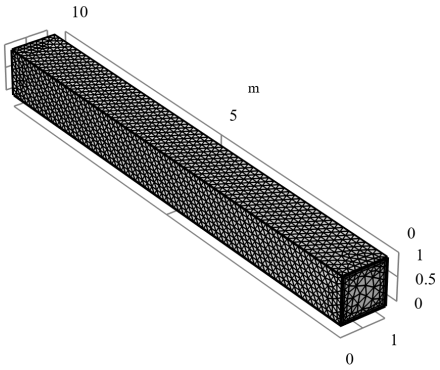

Figure 16. Geometric model for numerical simulation

Figure 16 depicts the geometric model for numerical simulation, which is a rectangular parallelepiped with a 1 m * 1 m square cross-section and a depth of 10 m. The total geometric volume is 10 m^3. A physical field control grid is employed to automatically divide the grid; it comprises 9083 grid vertices and includes 20272 tetrahedra, 8936 prisms, and 29208 elements. The average element quality is 0.6908, and the element volume ratio is 0.01277.

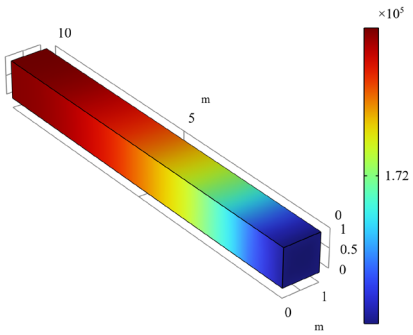

Figure 17. Contour plot of pressure (Unit: Pa)

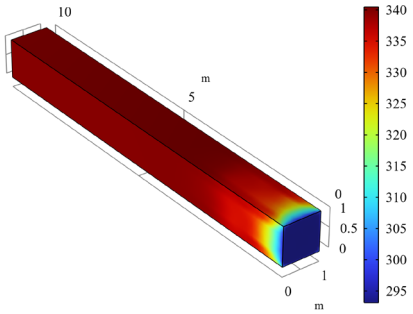

Figure 18. Contour plot of temperature(Unit: K)

Figure 17 shows the pressure contour map at the final moment, specifically at 60 s. The average absolute pressure of the vessel is 171997.602 Pa. According to Table 3, the theoretical calculation yielded 171977.6 Pa, which is in good agreement with the experimental value. Figure 18 illustrates the temperature contour maps at the final moment and at 60 s. The average temperature of the vessel is 332.22 K. According to Table 3, the theoretically calculated value is 332.15 K, which is in good agreement with the experimental result. This agrees with the theoretical and numerical models used in the present study.

To facilitate comparison between the results of the theoretical calculations and the numerical simulations, we plotted the pressure and temperature variations during the inflation phase, as shown in Figures 19 and 20. Subfigure (a) shows the global variation graph, whereas subfigure(b) shows the local magnification. Observations reveal that the discrepancy between theoretical calculations and numerical simulations is minimal, and the two are almost perfectly aligned. Differences between theoretical and simulated values for pressure and temperature are less than 0.02% and 0.03%, respectively, thereby verifying the accuracy of both theoretical calculations and numerical simulations.

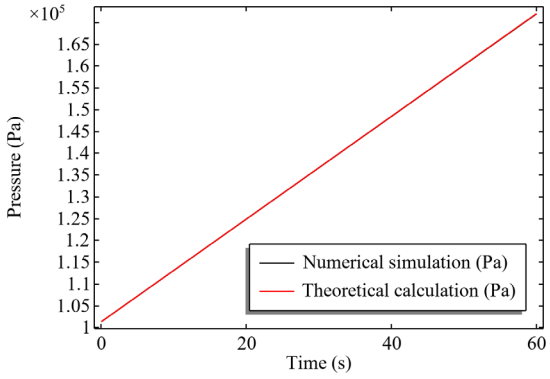

(a) Global variation

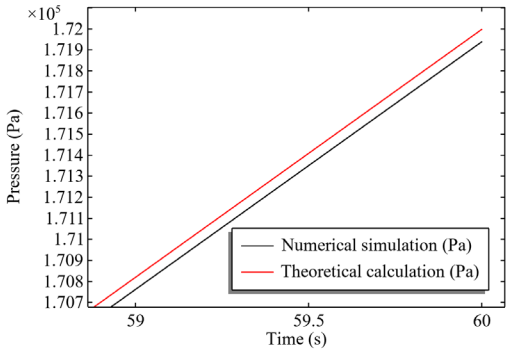

(b) Local magnification

Figure 19. pressure variation diagram of the VAC model

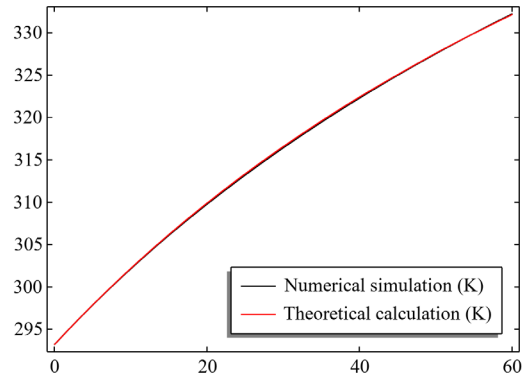

(a) Global variation

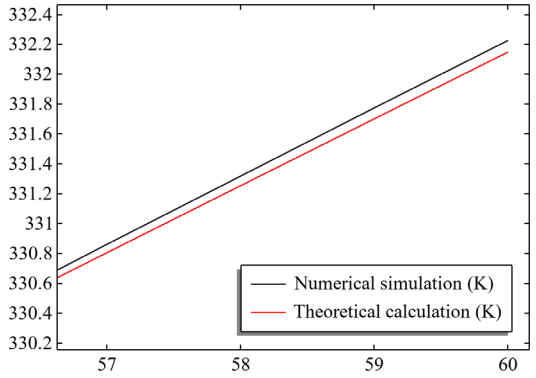

(b) Local magnification

Figure 20. temperature variation diagram of the VAC model

5. Discussion

5.1. Deep thinking of case analysis

Through theoretical derivation and case analysis, further research can reveal the following:

1. In the isochoric model, variations in both pressure and temperature are relatively large. In the isobaric model, the pressure and temperature remain unchanged from their initial states. Therefore, if system stability is a priority, as in underground gas storage facilities, the isobaric storage model is preferable because it offers higher energy storage efficiency and reduces energy loss.
2. The isothermal model involves slow charging and discharging, with sufficient heat transfer to the environment. To minimize energy loss, an adiabatic model with rapid charging and discharging is preferable.
3. The heat transfer model also includes heat exchange with the environment. To reduce energy loss, a lower convective heat transfer coefficient is preferable. When the heat transfer coefficient is zero, the heat transfer model degenerates into an adiabatic model. An adiabatic model is generally considered a better choice for energy conservation.
4. The charging pressure is generally higher than the internal pressure of the vessels. During discharge, the discharge pressure reflects the vessels' internal pressure and is typically higher than ambient pressure.
5. In an isochoric, adiabatic model, if the charging temperature does not significantly fall below the original gas temperature in the vessel, the charging process typically acts as heating.
6. Except for an isothermal model the higher charging temperature leads to increased final temperatures When the ambient temperature exceeds the internal temperature of a vessel, heat is absorbed, causing the vessel's internal temperature to rise.

5.2. Engineering implications of thermodynamic models

Based on the case analysis presented in the previous section and consideration of practical engineering applications, the 18 thermodynamic models established in this study provided significant guidance for engineering practice. The quantitative comparative results presented in the previous section (see Table 3) not only reveal differences in the thermodynamic behavior of gas vessels under various constraints, but also provide direct theoretical foundations for safety assessments, design optimization, and the formulation of operational strategies in industrial practice. The engineering implications of these thermodynamic models are systematically elaborated below from three perspectives: safety, design recommendations, and operational constraints.

Safety Implications. Section 4 illustrates that the isochoric adiabatic model experiences significant temperature fluctuations (143.58K, ranging from 188.57K to 332.15K) that endanger the material integrity. Metal containers are subject to thermal fatigue, low-temperature embrittlement or excessive thermal stress at connections and support during repeated cycles between -84.58 °C and 59 °C. On the contrary, the isochoric heat transfer model results in a temperature change of only 35.29 K in the discharging process, which effectively reduces the risk of thermal stress. The fast-refueling process for hydrogen energy applications is close to adiabatic process with temperature increase of up to 332.15K that may accelerate the degradation of materials or activate safety-relief devices. Therefore, pre-cooling systems or controlled filling rate are necessary in practice to approach the isothermal conditions.

Design Recommendations. A comparative analysis provides quantitative criteria for selecting constraints in different application scenarios. Isobaric models are better for underground gas storage facilities or large-scale compressed air energy storage systems where pressure stability is very important. They maintain constant pressure and temperature by changing the volume by 4.98 m 3. Hence, there is no pressure-cycling fatigue on the containment structures. There-

fore, flexible boundary designs such as piston separators or constant pressure caverns are needed. In applications where space is limited, such as on-board hydrogen storage tanks in ships, isochoric designs are required. But designers have to trade-off between heat transfer and adiabatic modes of operation, depending on how fast the system is running. Better heat transfer systems should be used in rapid-refueling stations to approximate isothermal conditions and avoid excessive temperature rise, for example. Slow industrial filling may be able to assume adiabatic conditions with adequate safety margins.

Operational limitations and enhancement. The analysis shows that operational protocols have a direct effect on the system's thermodynamic response characteristics. The heat transfer coefficient is a critical control parameter: when this coefficient approaches zero, the system behaves adiabatically with extreme temperature variations; when it is sufficiently large, the system approaches isothermal conditions. Therefore, operators can optimize the system response by adjusting external cooling or insulation measures. Furthermore, charging and discharging rates determine the validity of the lumped-parameter assumptions: rapid processes may induce spatial gradients requiring a distributed analysis, whereas slow processes satisfy the uniformity assumptions. In the isochoric adiabatic model, discharge must be terminated when the pressure approaches ambient pressure, to prevent vacuum conditions that could cause vessel collapse or contamination due to air pressure.

5.3. Limitations and applicability of thermodynamic models

5.3.1. Limitations of the present models

The 18 thermodynamic models developed in this study are based on several key assumptions that constitute their limitations. These limitations can be categorized into two groups: four fundamental, assumption-based limitations and three practical limitations related to experimental validation and physical phenomena that are not captured by the ideal-gas framework.

First, the ideal gas assumption is adopted. The current models assume that gases follow the ideal gas equation of state, with the compressibility factor Z equal to 1. This assumption is accurate at moderate pressures, especially when the pressure is less than 20 MPa and the temperature is more than 1.5 times the critical temperature. The compressibility factor Z can be very different from one for high-pressure hydrogen storage, like 70 MPa onboard tanks. For example, at 298 K, Z can be about 1.4. This means that the ideal gas assumption could lead to pressure predictions that are off by 15% to 25%. Under these conditions, equations of state for real gases, like the Peng-Robinson and Benedict–Webb–Rubin equations, are very important.

Second, the assumption of lumped parameters is made. The models use a lumped-parameter approach and assume that temperature, pressure, and density are evenly spread out throughout the vessel. To do this, the vessel needs to be small or have strong internal mixing. There may be big differences in temperature or pressure in large gas storage facilities like underground gas storage or tube trailers. To get accurate simulations, you need to use distributed parameter models or computational fluid dynamics methods.

Third, the idea that the mass flow rate stays the same. The models assume constant mass flow rates during charging and discharging. In practice, mass flow rates are affected by valve opening and flow resistance and may vary with time. Furthermore, the present models do not account for the effects of the charging jets on local heat transfer and mixing.

Fourth, we assume a constant heat transfer coefficient. The heat transfer models assume constant convective heat transfer coefficients during the process. Heat transfer coefficients depend on the fluid flow regime, temperature difference, and vessel geometry, and may vary as the process proceeds.

In addition to the four assumption-based limitations mentioned above, the present models have three additional practical limitations.

Fifth, lack of experimental validation. The present models are based entirely on theoretical derivations and numerical verifications without direct comparisons with experimental data. Future work requires measurements of temperature and pressure transients from instrumented pressure vessels to validate model accuracy.

Sixth, the Joule-Thomson effect was not considered. The present models assume ideal gas behavior, where the Joule-Thomson coefficient is zero, indicating that no temperature change occurs during isenthalpic throttling (Joule-Thomson expansion). This is fundamentally different from an ideal adiabatic expansion, in which temperature changes result from work extraction. However, in the case of real gases, especially at high pressures, the Joule-Thomson effect can cause additional cooling or heating upon discharge, which depends on the inversion curve. This behavior is not considered in the notion of ideal adiabatic expansion. This difference is important for the accurate prediction of temperature in high pressure situations.

Seventh, neglect of condensation and frost effects. The present models assume single-phase ideal gas behavior throughout the entire process. However, in the isochoric adiabatic discharging model, temperatures can drop to 188.57 K (-84.58 °C), which is above the condensation temperatures of air components (oxygen at 90.2 K and nitrogen at 77.4 K) at atmospheric pressure. For applications involving moist gases or temperatures below -40 °C, phase change effects, frost formation, and multiphase thermodynamics must be considered. The models should be extended to include real-fluid behavior and phase equilibrium calculations for such extreme conditions.

5.3.2. Applicability of the present models

Despite these limitations, the present models are applicable to the following engineering scenarios.

First, preliminary design of moderate-pressure gas storage systems. For compressed air energy storage systems, industrial gas tanks, and gas storage facilities operating at atmospheric to moderate pressures (below 20 MPa), the error introduced by the ideal gas assumption remains within acceptable limits, and the models can be used for rapid prediction of thermodynamic behavior.

Second, engineering analysis of rapid charging and discharging processes. In applications such as fast refueling at hydrogen stations or rapid response in compressed air energy storage systems, the charging and discharging times are relatively short, and the lumped-parameter assumption is generally valid. The models can be used to evaluate extreme temperature and pressure conditions, thereby providing guidance for material selection and safety assessments.

Thirdly, comparative studies are made under different thermodynamic constraints. In this study, the impact of isochoric versus isobaric constraints and adiabatic versus isothermal processes on the performance of the system is systematically investigated. Such horizontal comparisons are useful for engineers to theoretically choose the appropriate modes of operation such as more stable isobaric modes or more understandable adiabatic modes.

Fourth, a sensitivity analysis of the parameters. The analytical solution forms allow for parametric sensitivity analysis which can be used to study the influence of parameters like ambient temperature, heat transfer coefficient or charging temperature on the final states without the need of performing numerous numerical simulations.

Fifth, Boundary conditions for detailed numerical simulations. The analytical solutions presented in this work can be used as boundary conditions or validation benchmarks for computational fluid dynamics or finite element analysis models, particularly for validation of the accuracy of the numerical codes or providing initial estimates.

6. Conclusion

The paper offers a complete theoretical framework for studying the thermodynamic properties of gas vessels under varied operational conditions. Based on the fundamentals of variable-mass thermodynamics, we systematically formulate 18 unique thermodynamic models that represent all combinations of isochoric and isobaric restrictions, heat exchange, adiabatic and isothermal processes, and charging, storage and discharging steps. For each model, analytical solutions exist in differential and algebraic form. This facilitates their direct use in engineering and parametric analyses.

Detailed case studies quantitatively show the effect of different constraints and thermal processes on a 10 m3 meter vessel under the same initial conditions. The largest variations are shown by the isochoric adiabatic model with temperatures in the range of 188.57 K to 332.15 K and pressures in the range of 0.96 atm to 1.7 atm. The isochoric heat transfer model achieves the same maximum pressure of 1.7 atm but the temperature varies less from 257.9 K to 293.19 K due to heat transfer from the environment. Isobaric models, such as isobaric heat transfer, isobaric adiabatic, and isobaric isothermal, on the other hand, keep the temperature at 293.15 K and the pressure at 1 atm, but the volume changes by 4.98 m^3. These quantitative comparisons demonstrate that mechanical constraints fundamentally determine the system response characteristics, whereas thermal boundary conditions significantly moderate the temperature extremes.

The main novelty of this study lies in three aspects. First, we show how to systematically derive thermodynamic models for gas vessels that work in different ways and at different times. Second, we give clear analytical solutions for all 18 models in both algebraic and differential forms. Third, we did case-specific analyses and checks, compared different models, and showed how changing the system's constraints changes its thermodynamic behavior in a big way.

In terms of model limitations, the current framework presumes ideal gas behavior (applicable for pressures under 20 MPa), utilizes a lumped-parameter approximation necessitating a uniform spatial distribution of properties, and assumes constant mass flow rates and heat transfer coefficients. These models are especially useful for preliminary design of moderate pressure gas storage systems such as compressed air energy storage (CAES) and industrial gas tanks; engineering analysis of fast charging-discharging processes; comparative studies under different constraints; parametric sensitivity analyses; and as boundary conditions for detailed computational fluid dynamics (CFD) simulations.

Future works should be devoted to experimental validation with instrumented pressure vessel measurements, extension to real gas phenomena with equations of state (e.g. Peng-Robinson) for high-pressure applications, consideration of cyclic charge-discharge processes and inclusion of distributed-parameter effects for large storage facilities. A comprehensive theoretical framework is presented and useful in decision-making for the improved design, efficient operation and performance enhancement of gas vessels in the energy and industrial fields.

Nomenclature

p	gas pressure, Pa or atm
V	gas volume, m^3
n	the amount of substance of a gas,mol
T	gas temperature,K or °C
R	universal gas constant, 8.314J/(mol·K)

Z	gas compression factor, which is conventionally 1 for an ideal gas.
m	gas mass,kg
t	time, s
E_{CV}	Total system energy, J or kJ
Q	heat, J or kJ
W	expansion work done on the surroundings,J or kJ
U	thermodynamic energy, J or kJ
E_{in}	the energy flowing into the system, J or kJ
E_{out}	the energy flowing out the system, J or kJ
$E_{leakage}$	the energy leaked from the system, J or kJ
$\dot{m}_{in}$	mass flow rate of charging, kg/s
$\dot{m}_{out}$	mass flow rate of discharging, kg/s
$\dot{m}_{leakage}$	mass flow rate of leakage, kg/s
g	gravitational constant, N/kg
Z_{in}	the height of the charging port, m
Z_{out}	the height of the discharging port, m
Q_{final}	the initial heat of the system, J or kJ
Q_{start}	the final heat of the system, J or kJ
$\dot{Q}$	heat flow per unit time, W or kW
W_{final}	the mechanical work of the system at the final moment, J or kJ
W_{start}	the mechanical work of the system at the start moment, J or kJ
h_{in}	the enthalpy of the gas flowing into the system, J or kJ
h_{out}	the enthalpy of the gas flowing out of the system, J or kJ
c_{in}	the kinetic energy of the gas flowing into the system, J or kJ
c_{out}	the kinetic energy of the gas flowing out of the system, J or kJ
T_0	the initial temperature of the system, K or °C
T_{in}	the temperature of the gas flowing into the system, K or °C
T_{out}	the temperature of the gas flowing out the system, K or °C
p_0	the initial pressure of the system, Pa or atm
p_{in}	the pressure of the gas flowing into the system, Pa or atm
p_{out}	the pressure of the gas flowing out the system, Pa or atm
m_0	the initial mass of the system, kg
m_{in}	accumulated mass of gas flowing into the system, kg
m_{out}	accumulated mass of gas flowing out the system, kg
$m_{leakage}$	accumulated mass of gas leaked from the system, kg
V_0	the initial volume of the system, m^3
V_s	specific volume, m^3
p_s	specific pressure, Pa or atm
T_s	specific temperature, K or °C
h_{amb}	convective heat transfer coefficient, $W/(m^2 \cdot K)$
A_{vessel}	surface area of vessel, m^2
T_{amb}	ambient temperature, K or °C
c_p	specific heat capacity at isobaric, kJ/(kg·K)
c_v	specific heat capacity at constant volume, kJ/(kg·K)
k	adiabatic index, which is generally 1.4.
VH model	Isochoric heat transfer model
VA mode	isochoric adiabatic model
VT model	isochoric isothermal model
PH model	isobaric heat transfer model
PA model	isobaric adiabatic model
PT model	isobaric isothermal model
VHC model	isochoric heat transfer and charging model
VHD model	isochoric heat transfer and discharging model
VAC model	isochoric adiabatic and charging model
VAD model	isochoric adiabatic and discharging model
VTC model	isochoric isothermal and charging model
VTD model	isochoric isothermal and discharging model
PHC model	isobaric heat transfer and charging model
PHD model	isobaric heat transfer and discharging model
PAC model	isobaric adiabatic and charging model
PAD model	isobaric adiabatic and discharging model
PTC model	isobaric isothermal and charging model
PTD model	isobaric isothermal and discharging model
VHS model	isochoric heat transfer and storage model
VAS model	isochoric adiabatic and storage model
VTS model	isochoric isothermal and storage model
PHS model	isobaric heat transfer and storage model
PAS model	isobaric adiabatic and storage model
PTS model	isobaric isothermal and storage model

Appendix

The analytical solutions for Sections 3.1 and 3.2 are provided in the appendix.

Authorship contributions

Kangyu Deng: Conceptualization, Methodology, Formal analysis, Writing – original draft, Writing – review & editing. Xiaopeng Li: Investigation, Data curation, Visualization, Writing – review & editing. Wantong Wang: Resources, Validation, Supervision, Writing – review & editing. All authors have read and agreed to the published version of the manuscript.

Data availability statement

The data supporting the findings of this study are available from the corresponding author upon reasonable request.

Conflict of interest

The authors declare that they have no known competing financial interests or personal relationships that could have appeared to influence the work reported in this paper.

Acknowledgement

The authors would like to express their sincere gratitude to the academic editor and anonymous reviewers for their constructive comments and valuable suggestions, which have significantly improved the quality and clarity of this manuscript.

Funding

No fund is received from any source to carry out present study.

References

[1] Fermi, Enrico. Thermodynamics. Courier Corporation; 2012.
[2] Gyftopoulos, Elias P., and Gian Paolo Beretta. Thermodynamics: foundations and applications. Courier Corporation; 2012.
[3] Bejan, Adrian. Advanced engineering thermodynamics. John Wiley & Sons; 2016.
[4] Moran, Michael J., et al. Fundamentals of engineering thermodynamics. John Wiley & Sons; 2010.
[5] Masaaf Y, Ait El Kadi Y, Baghli F Z. Levelized cost of energy and storage of compressed air energy storage with wind and solar plants in Morocco. Journal of Thermal Engineering 2024; 10(4): 847-856. https://doi.org/10.14744/thermal.0000836
[6] Karagöz Y, Köten H. EFFECT OF DIFFERENT LEVELS OF HYDROGEN. JOURNAL OF THERMAL ENGINEERING 2019; 5(2). https://doi.org/10.18186/thermal.531704
[7] Wu Peiyi, Ma Yuan. Thermodynamics of Variable Mass Systems and Its Applications. Higher Education Press; 1983.
[8] Surana K. A more complete thermodynamic framework for fluent continua. Journal of Thermal Engineering 2015; 1(6). https://doi.org/10.18186/jte.00314
[9] Tong Jungeng, Wang Liwei, Ye Qiang. Engineering Thermodynamics. 6th Edition. Higher Education Press; 2022
[10] Chen Zesaos. Advanced Engineering Thermodynamics. 3rd Edition. University of Science and Technology of China Press; 2014
[11] Ning Chenxiao Introduction and Improvement of Pneumatic Technology. Chemical Industry Press; 2017
[12] Cheng Daxian. Mechanical Design Manual: Single Volume. Pneumatic Transmission. 5th Edition. Chemical Industry Press; 2010
[13] Xue L, Deng J, Wang X, et al. Numerical simulation and optimization of rapid filling of high-pressure hydrogen storage cylinder. Energies 2022; 15(14): 5189. https://doi.org/10.3390/en15145189
[14] Zhang E, Zhao Y, Zhang J, et al. Numerical analysis of hydrogen behavior inside hydrogen storage cylinders under rapid refueling conditions based on different shapes of hydrogen inlet ports. Energies 2024; 17(20): 5116. https://doi.org/10.3390/en17205116
[15] Li J Q, Li J C, Wang X Y, et al. A theoretical study on the hydrogen filling process of the on-board storage cylinder in hydrogen refueling station. Results in Engineering 2023; 18: 101168. https://doi.org/10.1016/j.rineng.2023.101168
[16] Zhang C, Cao X, Bujlo P, et al. Review on the safety analysis and protection strategies of fast filling hydrogen storage system for fuel cell vehicle application. Journal of energy storage 2022; 45: 103451. https://doi.org/10.1016/j.est.2021.103451
[17] Wu X, Liu J, Shao J, et al. Fast filling strategy of type III onboard hydrogen tank based on time-delayed method. International Journal of Hydrogen Energy 2021; 46(57): 29288-29296. https://doi.org/10.1016/j.ijhydene.2021.01.094
[18] Zhang Y, Yang K, Li X, et al. The thermodynamic effect of air storage chamber model on advanced adiabatic compressed air energy storage system. Renewable Energy 2013; 57: 469-478. https://doi.org/10.1016/j.renene.2013.01.035
[19] Raju M, Khaitan S K. Modeling and simulation of compressed air storage in caverns: A case study of the Huntorf plant. Applied energy 2012; 89(1): 474-481. https://doi.org/10.1016/j.apenergy.2011.08.019
[20] Li Xuemei. Research on the Influence of Component Characteristics on the Performance of Advanced Adiabatic Compressed Air Energy Storage System. University of Chinese Academy of Sciences(Institute of Engineering Thermophysics), 2015
[21] Sarmast S, Fraser RA, Dusseault MB. Performance and cyclic heat behavior of a partially adiabatic Cased-Wellbore Compressed Air Energy Storage system. Journal of Energy Storage 2021; Dec 1;44:103279. https://doi.org/10.1016/j.est.2021.103279
[22] Giannetti N, Milazzo A, Saito K. Thermodynamic investigation of asynchronous inverse air cycle integrated with compressed-air energy storage. Journal of Energy Storage 2022; Jan 1;45:103750. https://doi.org/10.1016/j.est.2021.103750
[23] Odukomaiya A, Kokou E, Hussein Z, Abu-Heiba A, Graham S, Momen AM. Near-isothermal-isobaric compressed gas energy storage. Journal of energy storage 2017; Aug 1;12:276-87. https://doi.org/10.1016/j.est.2017.05.014
[24] Stanek B, Ochmann J, Bartela Ł, Brzuszkiewicz M, Rulik S, Waniczek S. Isobaric tanks system for carbon dioxide energy storage–The performance analysis. Journal of Energy Storage 2022; Aug 1;52:104826. https://doi.org/10.1016/j.est.2022.104826
[25] Pottie D, Cardenas B, Garvey S, Rouse J, Hough E, Bagdanavicius A, Barbour E. Comparative analysis of isochoric and isobaric adiabatic compressed air energy storage. Energies 2023; Mar 10;16(6):2646. https://doi.org/10.3390/en16062646
[26] Shimin Z. The graphical representation of equilibrium for the isothermal and isobaric reactions of ideal gases. Journal of Mathematical Chemistry 2005; Aug;38(2):129-40. https://doi.org/10.1007/s10910-005-4838-5

[27] Corti DS. Isothermal-isobaric ensemble for small systems. Physical Review E 2001; Jun 26;64(1):016128. https://doi.org/10.1007/s10910-005-4838-5

[28] Baltazar SE, Romero AH, Rodríguez-López JL, Terrones H, Martoňák R. Assessment of isobaric-isothermal(NPT)simulations for finite systems. Computational materials science 2006; Oct 1;37(4):526-36. https://doi.org/10.1016/j.commatsci.2005.12.028

[29] Phuoc TX, Massoudi M. Pumping gaseous CO2 into a high-pressure, constant-volume storage cylinder: A thermodynamics analysis. Journal of Energy Storage 2021; Aug 1;40:102706. https://doi.org/10.1016/j.est.2021.102706

[30] Luo H, Xin Q, Yao C, Li C, Yang T, Wu X, Chahine R, Xiao J. Effect of Real Gas Equations on Calculation Accuracy of Thermodynamic State in Hydrogen Storage Tank. Applied Sciences 2025; Oct 17;15(20):11151. Applied Sciences, 15(20),11151. https://doi.org/10.3390/app152011151

[31] Hou Z, Jin K, Zhang S, Zhang H, Jiang Y, Sun J. Thermodynamic model for transient discharge of high-pressure hydrogen in storage tanks based on behaviors of ideal and real gases. International Journal of Hydrogen Energy 2026; Jan 5;197:152619. https://doi.org/10.1016/j.ijhydene.2025.152619

[32] Datta D. Thermodynamic Properties and Equations of States. Chemical Engineering Essentials 1: Comprehensive Chemical Engineering 2025; 8: 79-102. https://doi.org/10.1002/9781394372348.ch4

[33] Nederstigt, P. Real gas thermodynamics. Delft University of technology; 2017

[34] Jaeschke M, Schley P. Ideal-gas thermodynamic properties for natural-gas applications. International journal of thermophysics 1995; 16(6):1381-92. https://doi.org/10.1007/BF02083547